Application of clustering and the Hungarian algorithm to the problem of consistent vortex tracking in incompressible flowfields

Stevens, P. R.R.J.; Sciacchitano, A.

DOI
10.1007/s00348-021-03265-w

Publication date
2021

Document Version
Final published version

Published in
Experiments in Fluids

Experiments in Fluids (2021) 62:173
https://doi.org/10.1007/s00348-021-03265-w

RESEARCH ARTICLE

Application of clustering and the Hungarian algorithm to the problem of consistent vortex tracking in incompressible flowfields

P. R. R. J. Stevens[1] · A. Sciacchitano[2]

Received: 18 December 2020 / Revised: 13 July 2021 / Accepted: 14 July 2021 / Published online: 25 July 2021

Abstract

The ability to track vortices spatially and temporally is of great interest for the study of complex and turbulent flows. A methodology to solve the problem of vortex tracking by the application of machine learning approaches is investigated. First a well-known vortex detection algorithm is applied to identify coherent structures. Hierarchical clustering is then conducted followed by a unique application of the *Hungarian* assignment algorithm. Application to a synthetic flowfield of merging Batchelor vortices results in robust vortex labelling even in a vortex merging event. A robotic PIV experimental dataset of a canonical Ahmed body is used to demonstrate the applicability of the method to three-dimensional flows.

Graphic abstract

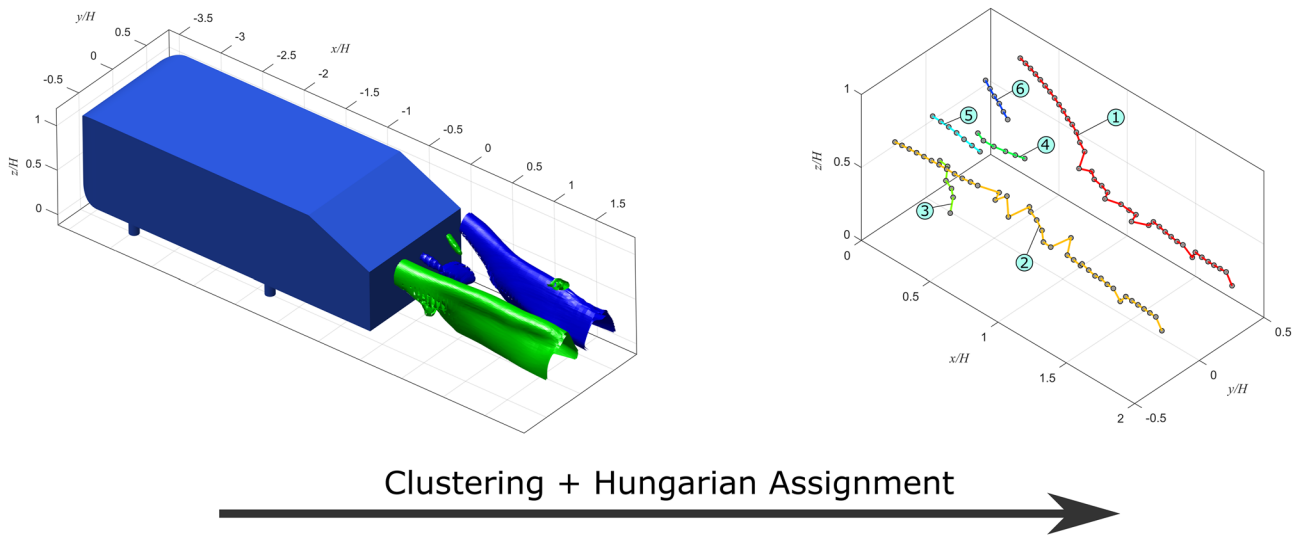

1 Introduction

Many aerodynamic flow fields of both academic and practical engineering interest are dominated by macro-scale vortex dynamics, which govern the evolution and interaction of coherent structures in turbulent flows (Lumley 1981). In the aircraft industry, understanding the vortex system produced by high-lift wing configurations is important for determining the minimum separation distance between aircraft during take-off and landing (e.g. de Bruin et al. 1996) and for identifying sources of airframe aerodynamic noise (e.g. Hardin

✉ P. R. R. J. Stevens
robbie.stevens@cantab.net

[1] Whiteways Technical Centre, Enstone, Oxfordshire OX7 4EE, UK

[2] Department of Aerospace Engineering, TU Delft, Delft, The Netherlands

and Wang 2003). In the auto-racing industry, the characterisation of complex vortex fields is key for enhancing car performance (e.g. Zhang et al. 2006).

Several studies have been dedicated to the definition and identification of vortices. In their seminal paper on the identification of a vortex, Jeong and Hussain (1995) define two requirements for a vortex core:

1. It must have a net vorticity, hence a net circulation.
2. Its geometry must be Galilean invariant.

Several vortex identification schemes have been proposed, which are typically classified into local and non-local (Cucitore et al. 1999). The former identify a vortex based on the value of local flow quantities, such as the static pressure [local pressure minimum, (Kline and Robinson 1990)] or the vorticity magnitude (Spalart 1988), or on the analysis of the velocity gradient tensor $\nabla\mathbf{u}$ (second invariant Q of $\nabla\mathbf{u}$, (Hunt et al. 1988); complex eigenvalues of $\nabla\mathbf{u}$, (Chong et al. 1990); second eigenvalue, λ_2 of $S^2+\Omega^2$, (Jeong and Hussain 1995); imaginary part λ_{ci} of the complex eigenvalue of $\nabla\mathbf{u}$ (Zhou et al. 1999). Non-local schemes instead rely on the idea of vortices as structures, which occupy a finite portion of space. These schemes range from the simple detection (non-Galilean invariant) based on closed or spiral pathlines or streamlines (Lugt 1979) to more advanced (Galilean invariant) approaches, relying on the tendency of two flow parcels to remain near each other (Cucitore et al. 1999). All these schemes enable the identification of vortical structures to some extent and have been proven successful under certain flow conditions. They do however present several limitations as discussed in detail in Jeong and Hussain (1995) and Cucitore et al. (1999), among others. Notably, those schemes have been devised mainly for isolated vortices and fail or are strongly intermittent in the presence of vortex interactions or small-scale turbulence. To overcome these issues, Graftieaux et al. (2001) introduced a new non-local vortex identification scheme, which enables determination of the centres and boundaries of vortex structures solely based on information from the topology of the velocity field and not its magnitude. The approach was proven for a turbulent swirling flow in a circular duct, but the problem of unsteady interaction between vortices was not addressed by the authors.

Machine learning (ML) algorithms are increasingly used in fluid mechanics to extract information from data, as demonstrated by the recent review of Brunton et al. (2019). Clustering is an unsupervised machine learning technique that identifies similar groups or *clusters* in the data. A few applications of clustering to fluid mechanics are reported in the literature: Kaiser et al. (2014) introduced a cluster-based reduced order modelling strategy for unsteady flows to identify physical mechanisms in an unsupervised manner; Amsallam et al. (2012) made use of clustering to partition the domain into regions, where local reduced-order bases were constructed. Deng et al. (2020) propose a method which first uses a normalised version of the *Instantaneous Vorticity Deviation (IVD)* metric of Haller et al. (2016) to describe vortex-like behaviour. They then use clustering to identify vortices. In this work, we propose the use of hierarchical clustering (Xu and Wunsch 2008) in combination with the vortex identification method of Graftieaux et al. (2001) to identify and track coherent structures from *2D* and *3D* PIV data even in the presence of unsteady interactions.

Recently there have been some great developments in the state-of-the-art methods used for vortex detection. Some significant advances in the use of *Deep Learning* for vortex identification are reported in Kim and Gunther (2019), Deng et al. (2019), Wang et al. (2020). While these methods have demonstrated exciting advances, there are concerns about the use of so-called *black-box* ML strategies, especially in the use of *Deep Learning*, where often the background process is difficult to explain. In addition, many of these style ML approaches are computationally very expensive and require large training datasets. In this paper, a practical vortex extraction and labelling/tracking procedure is proposed, which is computationally inexpensive and does not require training (unsupervised machine learning approach). While variations on the proposal can be made (e.g. different vortex extraction methods), the use of the Hungarian algorithm for consistent vortex labelling is the unique contribution of this work.

Gunther and Theisel (2017) summarise traditional vortex extraction methods and distinguish them depending on reference frame invariance and whether they are region-based, line-based, geometry-/integration-based and boundary extraction approaches. The interested reader is referred to their excellent discussion of the advantages and disadvantages of the respective techniques. The technique described in this paper is intended to be one effective way to reliably track vortices and label them consistently when data is in slice form. The approach as proposed can be summarised as follows:

- Apply a Galilean-Invariant, region-based method (γ_2 is demonstrated) to extract vortex features present in 2D slices of the flow (such slices can be in the spatial sense or time instances).
- Deploy hierarchical clustering to help accurately determine vortex centres even under complicated flow phenomena such as merging or imperfect vortex core boundary definitions.
- Use *Hungarian assignment* to consistently label vortices between slices while accounting for vortices merging or disappearing/bursting.

It is found that this approach is useful and practical when used with experimental datasets. The consistent labelling which is achieved by *Hungarian assignment* only requires an input of the coordinates of a vortex centre and is not therefore dependent upon the specific vortex detection or vortex centre determination method.

2 Background of vortex identification and machine learning

This section briefly discusses the theoretical background of the vortex identification scheme, hierarchical clustering and *Hungarian assignment*. It should be noted that the approaches described herein are considered at a macro-vortex scale as might occur in the aforementioned applications; however the techniques are independent of scale and could equally be applied to different length scales.

2.1 Graftieaux's method

Graftieaux et al. (2001) define a Galilean invariant, non-local method which does not rely on $\nabla\mathbf{u}$. This is immediately advantageous when experimental data such as PIV is concerned where any noise in the measurement can be amplified by differentiating the flowfield. Graftieaux et al. showed that for a 2D, incompressible, velocity field defined on a regular grid space, an approximation of a vortex core boundary can be found using the following relationship:

$$\gamma_2 = \frac{1}{N}\sum_{S}\frac{[\mathbf{PM}\wedge U_c]\cdot z}{||\mathbf{PM}||\cdot||U_c||} \tag{1}$$

In this notation $\mathbf{U_c} = U_M - \tilde{U}_P$, where $\mathbf{U_M}$ is the velocity vector at a given node $\mathbf{M}$ and $\tilde{\boldsymbol{U}}_\mathbf{P}$ is the local advection velocity at point $\mathbf{P}$. $\mathbf{PM}$ is a radius vector and $\mathbf{z}$ is a unit normal. N is the number of nodes inside a given area S. The wedge product, $\mathbf{PM}\wedge\mathbf{U_c}$ is a bi-vector which gives the area an orientation and hence allows the sense of vortex rotation to be extracted. Figure 1 shows the generalised vector arrangement for a simple case. Contour nodes, m_n are coincident with regular grid nodes. For an axi-symmetric vortex it is trivial to show that for a given radial distance from the vortex centre, $\mathbf{PM}=\langle\mathbf{PM_n}\rangle$ and $\mathbf{U_c}=\langle U_{c_n}\rangle$, where n is the number of grid nodes at a given radius. In more realistic flow conditions, this assumption is generally not valid, due to vortex asymmetry or shear instabilities for example.

There are a number of limitations to the applicability of the γ_2 method in the general case. Firstly the method as defined in the bi-vector sense operates on a 2D, solenoidal (divergence free) 'slice' of a fluid flow. Secondly the slice direction can have a profound influence on the ability to correctly identify vortices. This is discussed more in Sect. 2.1.1.

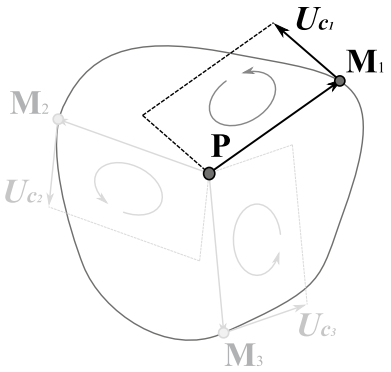

Fig. 1 2D interpretation of γ_2

Thirdly, the γ_2 method takes a $2/\pi$ contour level which represents a theoretical viscous vortex core, which may be imperfect when applied to finite and real experimental data. It should be noted that, while the γ_2 method is used as the input to the clustering and *Hungarian* process here, the clustering and *Hungarian* process could equally be applied to any other method that extracts vortex centres.

2.1.1 Influence of slicing direction

To process a 3D flowfield with γ_2, it must be sliced. The vortex identification can be influenced by the choice of slice direction. Ideally the slice should be perpendicular to the vortex axis. This however is not a very realistic expectation for general flowfields where the vortex axis could be tilted relative to the slice direction. In addition, if the flowfield has several vortices, it is not realistic to expect that all the vortices have an axis perpendicular to the vortex axis. Simpson et al. (2018) investigated this problem for stereo PIV data by performing a numerical simulation on an isolated Lamb-Oseen vortex. They first simulated a vortex with no axial velocity then applied a Gaussian distribution of axial velocity centred on the vortex axis to provide a more realistic case. They indicate that in both cases the circulation curve is stretched in the radial direction although ultimately asymptotes to the correct value and the apparent radius of the vortex core is overestimated, leading to an enlargement of the vortex core. It seems that these effects are relatively small, even for large relative angles (between the slice and vortex axis) of up to 40°. They do suggest however that if there is vorticity associated with the axial flow distribution such as when a Gaussian axial velocity distribution is applied then there can be a sizeable error in the vortex centre location. Simpson et al. (2018) showed that the positional error displays an approximately linear relationship with increasing angle between the slice and the vortex axis in the range of ±40°. Their study showed that error can be as large as 10% (of the core radius value) at a 20° angle. While it is not the

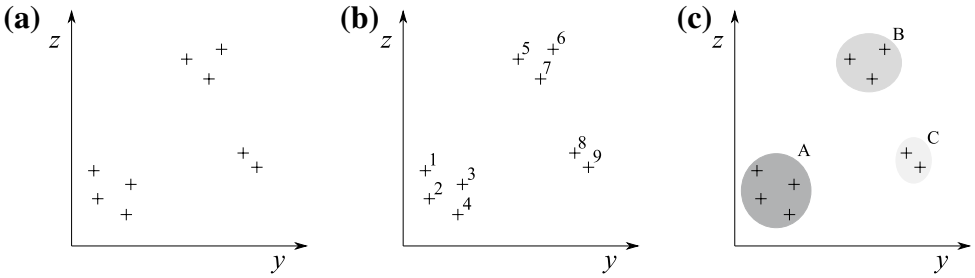

Fig. 2 Hierarchical clustering (**a**) Input data with unclassified objects, (**b**) objects labelled numerically and (**c**) objects with similar properties clustered together

intent of the present study to investigate this phenomenon, it is nevertheless recommended that when using γ_2 the slice direction should have a small angle relative to the vortex axis or alternatively for the determination of the vortex centre, the vectors could be interpolated onto an inclined plane in a similar way to that proposed by Simpson et al. (2018) (assuming 3D vector information is available).

2.2 Hierarchical clustering

One of the most challenging parts of coherent structure tracking and characterisation is concerned with occurrences of vortex interaction. A simple example is when vortices undergo a merging process. Clustering is one way to group coherent structures together.

A simple example of the clustering philosophy is given in Fig. 2. An input dataset of unclassified objects (Fig. 2a) are labelled numerically (Fig. 2b) and objects with similar properties are *clustered* together (Fig. 2c). There are a range of methods available to achieve this. The approach discussed herein is a modified version of a basic *single-link* hierarchical cluster analysis (Sibson 1972).

The single-link clustering used here is agglomerative i.e. it seeks to combine objects with similar properties. The objects used here are the centroids of the γ_2 contours. There must be some approach to decide which centroid datapoints should be joined into a cluster. Here, a calculation of the squared Euclidean distance (Spencer 2013) of each centroid coordinate point relative to all the others is conducted first. The squared Euclidean distance is chosen as it is generally accepted as a reliable distance metric. This could however be defined in several alternative ways e.g. Euclidean distance, Manhattan distance or Mahalanobis distance. There can be a difference in relative distance extracted between these methods e.g. the Manhattan distance will by definition always be greater than the Euclidean distance.

The linkage criterion determines how close clusters of γ_2 contour centroids can be before they are classified as part of the same cluster. This linkage distance $D(A, B)$ is described by the minimum between elements of each

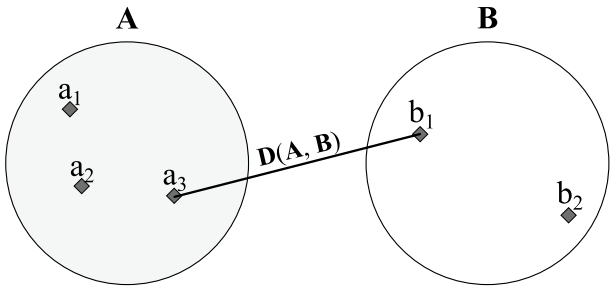

Fig. 3 Linkage distance for single-link maximum cluster similarity. Adapted from Manning et al. (2008)

cluster i.e. those with the maximum similarity. This is depicted in Fig. 3 and described mathematically by Eq. 2.

$$D(A,B) = \min_{a \in A, b \in B} d(a,b) \tag{2}$$

In practice the user needs to set some distance threshold for how close contour centroids can be to each other to be considered as part of the same cluster. The choice of this threshold is critical as you want it to be large enough to allow robust distinction between clusters that represent different vortices yet small enough to distinguish vortices from one another when they are in close proximity. In practice the clusters which occur due to vortices are relatively distinct and this threshold value does not seem to be sensitive. It was found that clustering proceeded effectively in the test cases when the product 0.6*average distance of all the other points relative to a datapoint was greater than the square root of the distance of the point that is furthest away from the original. If the threshold was exceeded then a new cluster gets formed and this proceeds until no more new clusters are created.

Hierarchical clustering works well in *2D*; however strong changes in circulation or other vortex parameters in space and time make the method difficult to handle in three dimensions. The next section introduces the *Hungarian* assignment approach which will later be used to allow robust temporal tracking of vortices in 2D and the calculation of 3D vortex trajectories.

2.3 Hungarian assignment

The *Hungarian algorithm* was derived by Kuhn (1955) as an approach to solving the *Assignment Problem*. The algorithm attempts to optimise the assignment of tasks to workers by minimising the total cost. The time complexity of the algorithm was shown to be strongly polynomial by Dinits (1970) and Edmonds and Karp (1972), making it ideal for rapid computation of large numbers of assignments, such as complex flows with many vortices.

Here the algorithm is applied to the problem of vortex trajectory tracking. Consider first the *2D* position change of a system of n vortices in time. A simple system of four vortices in time is shown in Fig. 4. The problem is how to create an automatic coupling of these vortices as they advect temporally. A *Hungarian* assignment formulation based on that of Munkres (1957) can be applied. It must first be assumed that at both time t and $t+1$ the locations of the vortices are known a priori. The a priori determination of vortex position can be achieved using the aforementioned γ_2 method in combination with hierarchical clustering. It is also helpful if the vortices are labelled. Here the vortices are labelled as set, $\zeta = \{A, B, C, D\}$ at time t and in paired order $\zeta' = \{F, H, G, E\}$ at time $t+1$. A cost matrix must then be defined. To define the cost matrix any vortex at time t can be selected as a hub. The Euclidean distance relative to the hub coordinate of each remaining vortex is calculated. For example if the hub is defined as vortex A then the Euclidean distance is calculated to the elements F, H, G and E, respectively, that make up the set ζ'. A maximum hub distance threshold can optionally be employed to help prevent erroneous assignment of vortices that are far apart. The hub is then changed to the next vortex and the process repeated until each vortex has acted as a hub at least once. For this example, the resultant cost matrix, M becomes:

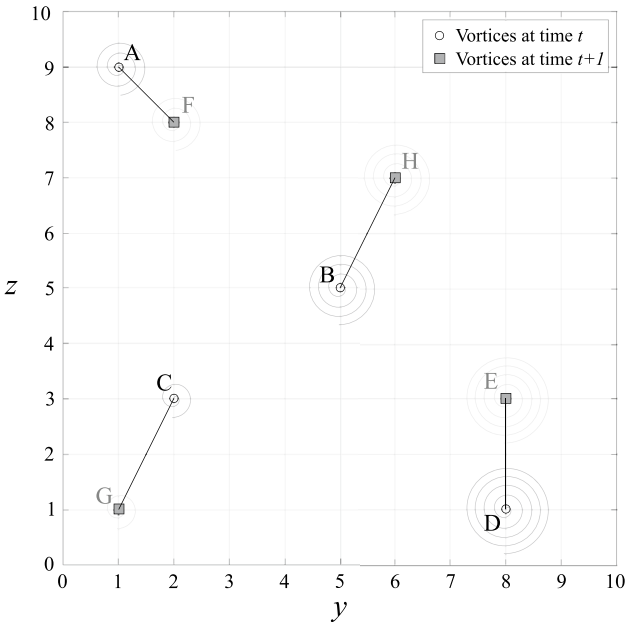

Fig. 4 Temporal advection of hypothetical four vortex system in *2D* space

$$\mathbf{M} = \begin{bmatrix} & E & F & G & H \\ A & \sqrt{85} & \sqrt{2} & 8 & \sqrt{29} \\ B & \sqrt{13} & \sqrt{18} & \sqrt{32} & \sqrt{5} \\ C & 6 & 5 & \sqrt{5} & \sqrt{32} \\ D & 2 & \sqrt{85} & 7 & \sqrt{40} \end{bmatrix} \tag{3}$$

The next step is to subtract the row minima:

$$\mathbf{M}' = \begin{bmatrix} \sqrt{85} & \sqrt{2} & 8 & \sqrt{29} \\ \sqrt{13} & \sqrt{18} & \sqrt{32} & \sqrt{5} \\ 6 & 5 & \sqrt{5} & \sqrt{32} \\ 2 & \sqrt{85} & 7 & \sqrt{40} \end{bmatrix} - \begin{bmatrix} \sqrt{2} \\ \sqrt{5} \\ \sqrt{5} \\ 2 \end{bmatrix} \tag{4}$$

This reduces to:

$$\mathbf{M}' = \begin{bmatrix} & E & F & G & H \\ A & (\sqrt{85}-\sqrt{2}) & 0 & (8-\sqrt{2}) & (\sqrt{29}-\sqrt{2}) \\ B & (\sqrt{13}-\sqrt{5}) & (\sqrt{18}-\sqrt{5}) & (\sqrt{32}-\sqrt{5}) & 0 \\ C & (6-\sqrt{5}) & (5-\sqrt{5}) & 0 & (\sqrt{32}-\sqrt{5}) \\ D & 0 & (\sqrt{85}-2) & 5 & (\sqrt{40}-2) \end{bmatrix} \tag{5}$$

Each of the vortices in set ζ' are assigned to the corresponding vortices in set ζ with the pairing indicated by the index locations of the null elements of the matrix M'; as a result, A pairs with F, B pairs with H, etc.

In this example there are only four vortices so the assignment is relatively intuitive and could even be conducted manually with a full *Hungarian* assignment, $\zeta \in \zeta'$. In an arbitrary vortex system however, the number of possible assignment combinations is $n!$, so with even a relatively small number of vortices, it becomes an untenable task to track vortex positions temporally or spatially by manual means.

The main assumption of the above approach is that the time step considered, Δt is selected such that no vortex travels more than half the minimum Euclidean distance between it and the nearest influencing vortex, $\delta/2$. This is shown in Fig. 5 for a simple case. If $I \subseteq \zeta$ and I represents a set of all possible positions of vortex I at time $t + \Delta t$, and II represents a set of all possible positions of vortex II at time $t + \Delta t$, then it follows that Δt is selected such that:

$$I \not\subset II \tag{6}$$

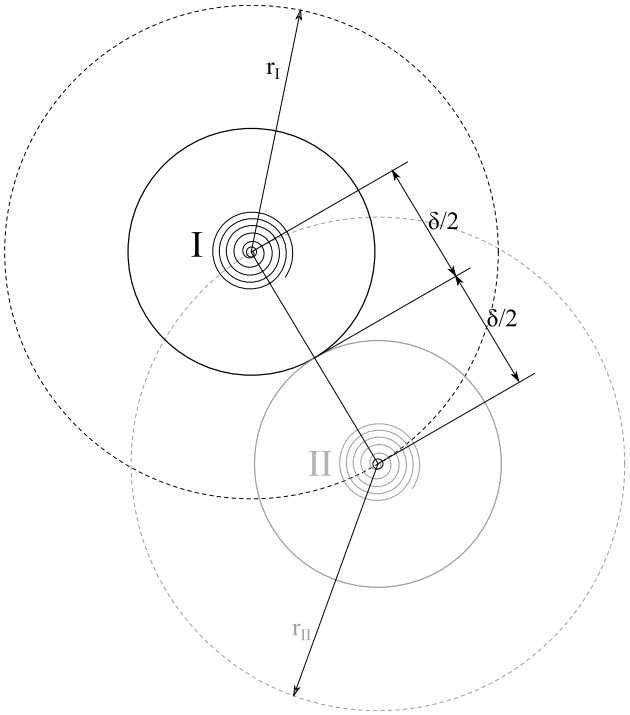

Fig. 5 Vortex separation limit. Here $\delta/2$ is the minimum Euclidean separation distance between vortices *I* and *II*. The radii r_I and r_{II} tend towards infinity and represent the possible range of motion of the vortex given infinite time

One way to enforce satisfaction of a unique assignment condition based on the Δt selection is to iteratively reduce the timestep until a unique set of assignments occurs. This requires the data to be sufficiently temporally resolved. In addition, to be considered as valid, the Euclidean vortex displacement measure must be above the noise level of the vortex spatial determination. In general, it is also the case that fluid physics has an effect on the minimum vortex separation as there is a limit to how close two initially separate vortices can be relative to one another before they are strongly influencing one another (considered merged for example), which is also linked to the vortex identification criterion used.

A real flow will experience phenomena such as vortex burst or vortex creation and there is also the possibility of vortices entering or leaving the field of view of interest. This is tackled simply by modifying the cost matrix accordingly. For example, consider the next step in time, *t+2* of the four vortex system. Here we assume that vortex *F* bursts such that $F \notin \zeta'$. We use the cost matrix to automatically label the burst vortex before continuing with the normal steps of the *Hungarian Algorithm*. Clearly if $\zeta = \emptyset$ then no *Hungarian* assignment can be carried out. The same process for 3D trajectory labelling is followed

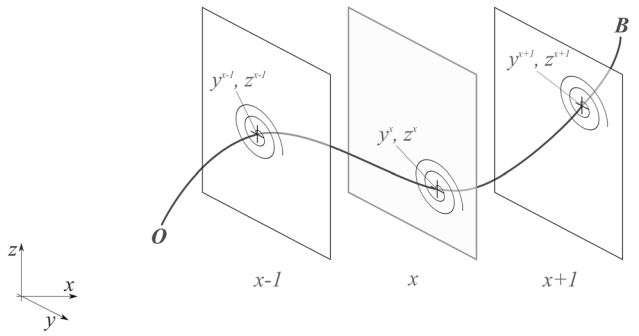

Fig. 6 Vortex advection in space

with the exception that slices of the flowfield in space (shown in Fig. 6) are used as opposed to slices in time.

3 Temporal vortex tracking example in 2D

Initial testing of the hierarchical clustering and *Hungarian* assignment algorithm in combination with the method of (Graftieaux et al. 2001) has been conducted on a synthetic, temporally evolving flowfield. This test flowfield is not representative of any physical flowfield. A merging phenomenon between two co-rotating vortices is induced after a short time. The flowfield is constructed from three *Batchelor* vortices advecting in a 2D plane. Each *Batchelor* vortex is defined as having an azimuthal velocity distribution according to the relationship (Batchelor 1964) (Fig. 7):

$$u_\theta = qW_0\left(1 - \exp\left(\frac{r}{r_{\text{core}}^2}\right)\right) \tag{7}$$

In this notation q is the swirl ratio, W_0 is the velocity scale defined as the delta between the vortex core axial velocity and the freestream and r is defined as the radius of a point from the centre of the vortex. The axial velocity profile is defined as:

$$u_{\text{axial}} = U_\infty + W_0 \cdot \exp\left(-\frac{r}{r_{\text{core}}}\right)^2 \tag{8}$$

The vortex properties defined at $t = 0$ s are summarised in Table 1. The vortex advection continues until $t = 5.6$ s. The freestream velocity is $U_\infty = 2$ ms^{-1} and dynamic viscosity $\mu = 1.81\ e^{-5}$ kg m^{-1} s^{-1}.

Consider two vortices in relatively close proximity to one another undergoing a merging phenomenon (such a phenomenon is seen in the time sequence of merging *Batchelor* vortices in Fig. 8). Non-local γ_2 contours are

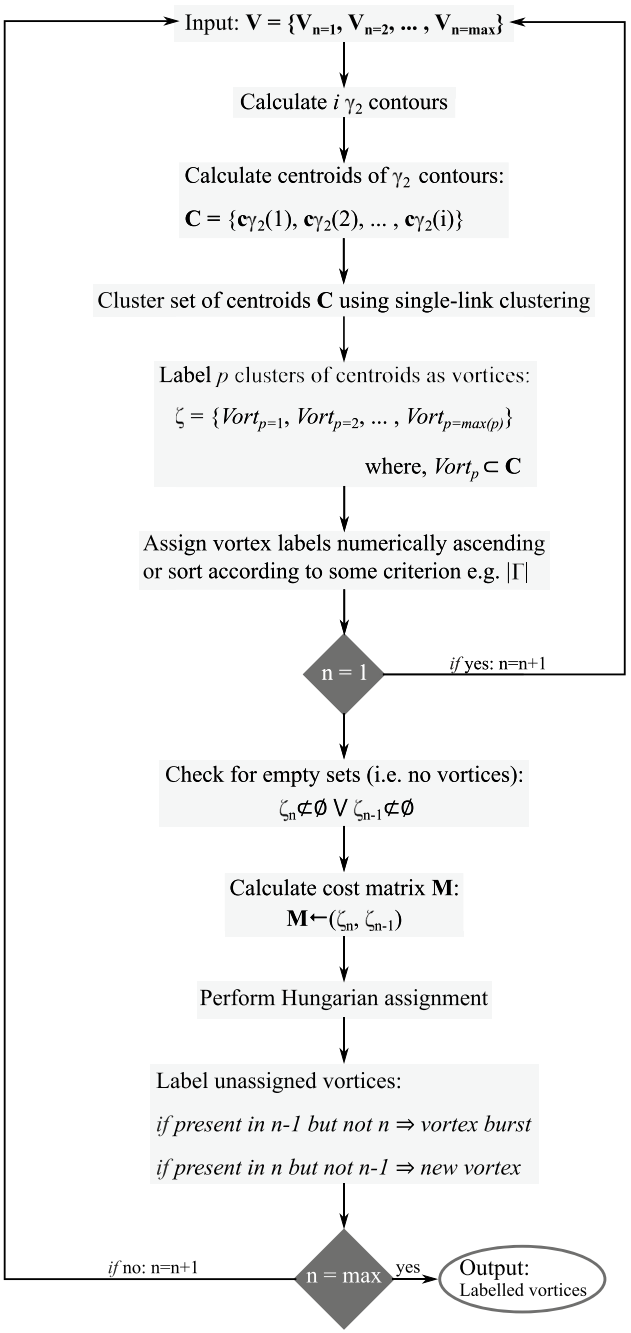

Fig. 7 Summary of proposed vortex tracking algorithm

calculated according to the approach outlined in 2.1. The axis of rotation of each vortex needs to be determined individually.

At time $t = 0.2$ the centroids of the γ_2 contours that define each vortex are approximately coincident and a mean of each *cluster* of centroid positions can be taken as a reasonably reliable indicator of the axis of vortex rotation. At time $t = 1.0$, the vortices labelled *Vortex 1* and *Vortex 3* are in close proximity and the γ_2 contours define a larger all encompassing *merged* vortex. This is not a big problem here since the vortices are of similar strengths but if not then this causes an erroneous bias in the vortex centroid position since the vortices have not fully merged. In this latter instance, the vortex centres can be much better defined as the mean centroids of the contours that are clustered together. This is discussed more in the next section but in this example it is clear that a paradox is formed, which can cause the calculation to essentially define three vortices, namely the original pair and one which encompasses both.

3.1 Vortex core centroid determination

The theoretical boundary of the vortex core is at $\gamma_2 = 2/\pi$ (Graftieaux et al. 2001). This is considered as a purely theoretical definition i.e. the contour level that corresponds to the peak azimuthal velocity. In an ideal vortex (e.g. theoretical isolated vortex), the centroids of all the γ_2 contour levels would be coincident. In practice with experimental data, the determination of the core level contour centroid can be a little noisy (especially between slices and if there are noisy artefacts in the data). It was thus found that to mitigate intra-slice centroid noise, one approach which gave more consistent results was to extract a range of γ_2 contours around each vortex, find the centroid of each and then deploy the clustering algorithm to identify vortex structures as represented by *clusters* of centroid data points. The effective vortex centre is then taken as the mean of the clustered points. This doesn't have an explicit physical meaning in itself; however in a merging event for example, a change in what datapoints constitute a cluster could manifest as a shift in the subsequent mean centroid position. This could be interpreted as an indicator of a physical merging event.

4 Experimental assessment

This section demonstrates an approach to constructing three-dimensional vortex trajectories by using the γ_2 method and hierarchical clustering to identify vortices in *2D* planes and

Table 1 Batchelor vortex properties

Vortex	x	y	r_{core}	u_θ/U_∞	u_{axial}/U_∞	u_{adv}/U_∞	v_{adv}/U_∞
1	0.45	0.6	0.09	15	5	0.0	− 2.5
2	0.2	0.3	0.09	− 15	5	7.5	2.5
3	0.7	0.5	0.09	15	5	− 7.5	0.0

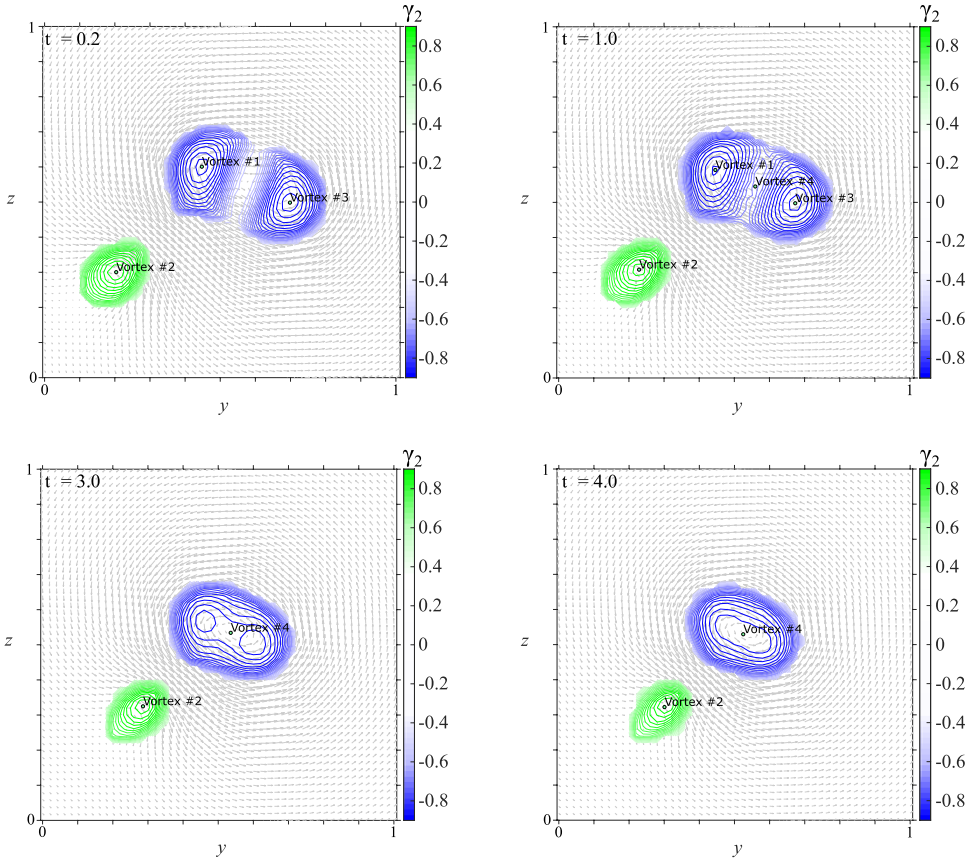

Fig. 8 Synthetic flowfield of Batchelor vortices merging. Anti-clockwise rotation is blue and clockwise is green. The γ_2 core is $2/\pi$ according to Graftieaux et al. (2001)

then *Hungarian assignment* to link vortices on upstream and downstream planes. The method is tested with a volumetric, experimental dataset, namely robotic PIV data of the vortex system on an *Ahmed* body (Fig. 9).

4.1 Experimental method

The proposed approach for vortex identification and tracking is assessed using the experimental data of the flow in the near wake of an Ahmed reference model (Ahmed et al. 1984). The experiments were conducted in the Open Jet Facility (OJF) of the TU Delft Aerodynamics Laboratories. The OJF is an open-jet closed-loop tunnel with an octagonal test section of 2.85×2.85 m^2, where a maximum free-stream velocity of 35 ms^{-1} can be reached with 0.5% turbulence intensity (Lignarolo et al. 2015). The model is a 1 : 2 replica of the original Ahmed reference model (Ahmed et al. 1984) with 25° slant angle; its dimensions are $L \times W \times H = 522 \times 194.5 \times 144$ mm^2. The experiments were performed at free-stream velocity of 12 ms^{-1}, yielding a Reynolds number of 115,000 based on the model's height.

The flow velocity measurements were carried out with the robotic volumetric PTV technique introduced by Jux et al. (2018), which makes use of a Coaxial Volumetric Velocimeter (Schneiders et al. 2018) manipulated by a *UR5* collaborative robotic arm from Universal Robots. The flow was seeded with sub-millimetre neutrally buoyant Helium-Filled Soap Bubble (HFSB) flow tracers

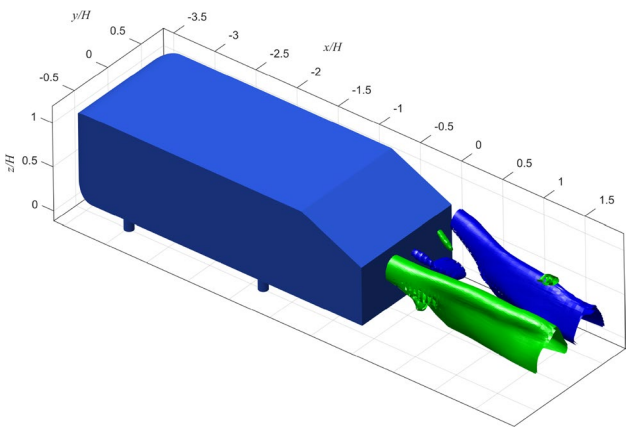

Fig. 9 Ahmed Body wake vortices represented as iso-surfaces of $\gamma_2 = 2/\pi$. Blue iso-surfaces represent counter-clockwise vortex rotation and green iso-surfaces represent clockwise vortex rotation when viewed from downstream

Table 2 Experimental parameters of the Ahmed body experiment

Seeding	Neutrally buoyant HFSB, ≈ 300 µm diameter
Illumination	Quantronix Darwin-Duo Nd:YLF laser (2 × 25 mJ @ 1 kHz)
Imaging device	LaVision MiniShaker S
	4 × CMOS cameras
	800x600 pixels @ 511Hz
	4.6 µm pixel pitch
Imaging parameters	$f = 4$ mm, $f\# = 8$
Measurement volume	$200 \times 200 \times 450$ mm^3
Acquisition frequency	$f_{acq} = 700$ Hz
Nominal magnification factor	≈ 0.01@40 cm distance
Number of images	8, 000

(Scarano et al. 2015), and the illumination was provided by a *Quantronix Darwin Duo Nd:YLF* laser and delivered by an optical fibre. The most relevant parameters of the experimental setup are summarised in Table 2; further details are reported in Sciacchitano and Giaquinta (2019). Image acquisition and processing was conducted with the *LaVision DaVis 8* software.

The raw images were pre-processed with a frequency high-pass filter (Sciacchitano and Scarano 2014) to reduce the effects of the unwanted laser light reflections. The pre-processed images were then analysed via the Shake-the-Box algorithm (Schanz et al. 2016). The tracks velocity information was successively averaged within Gaussian-weighted cubic bins of $20 \times 20 \times 20$ mm^3 to retrieve the time-averaged flow velocity, following the approach proposed by Agüera et al. (2016). Finally, a solenoidal filter (Azijli and Dwight 2015) was applied to the time-average velocity field to impose conservation of mass for incompressible flows, thus reducing the contribution of measurement noise.

4.2 Experimental results

The Ahmed body with iso-surfaces of $\gamma_2 = 2/\pi$ superimposed is shown in Fig. 9. Blue iso-surfaces represent counter-clockwise vortex rotation and green iso-surfaces represent clockwise vortex rotation when viewed from downstream. A representation of the labelled vortex trajectories is shown in Fig. 10. A numeric label is assigned to each vortex. The two dominant wake vortices are labelled as *vortex 1* and *vortex 2*. Additional vortices in the near-body region of the wake are also identified. While the primary vortices are well-recognised for an Ahmed body, the authors acknowledge that different vortex detection schemes may result in different numbers of vortices being detected in the flowfield. Here we have demonstrated that despite the complex nature of the near-body vortex system, the *Hungarian* assignment ensures robust demarcation and labelling.

Slices of the γ_2 fields are compared in Fig. 11. Vortex centres are shown as the centroid of the smallest contour of each vortex. A limitation in the γ_2 method is apparent when studying the contours in these slices. Clipping of the lower part of the dominant vortices is observed at $x/h = 0.818$, $x/h = 0.951$ and $x/h = 1.262$. This is due to the windowing that the γ_2 method uses. The amount of clipping here amounts to approximately $z/H = 0.1$ from the edge of the data domain.

While γ_2 is used in this demonstration as it is a popular vortex identification technique for slice data, it is emphasised that the *Hungarian* labelling and tracking approach could equally be applied in combination with several other vortex identification schemes.

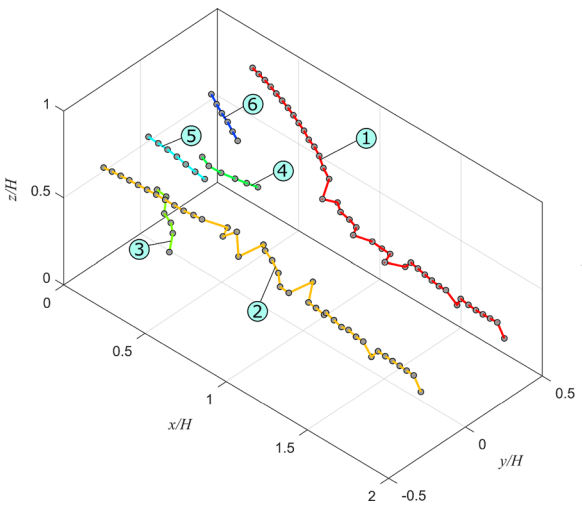

Fig. 10 Ahmed body wake vortices represented as labelled trajectories of γ_2 contour centroids

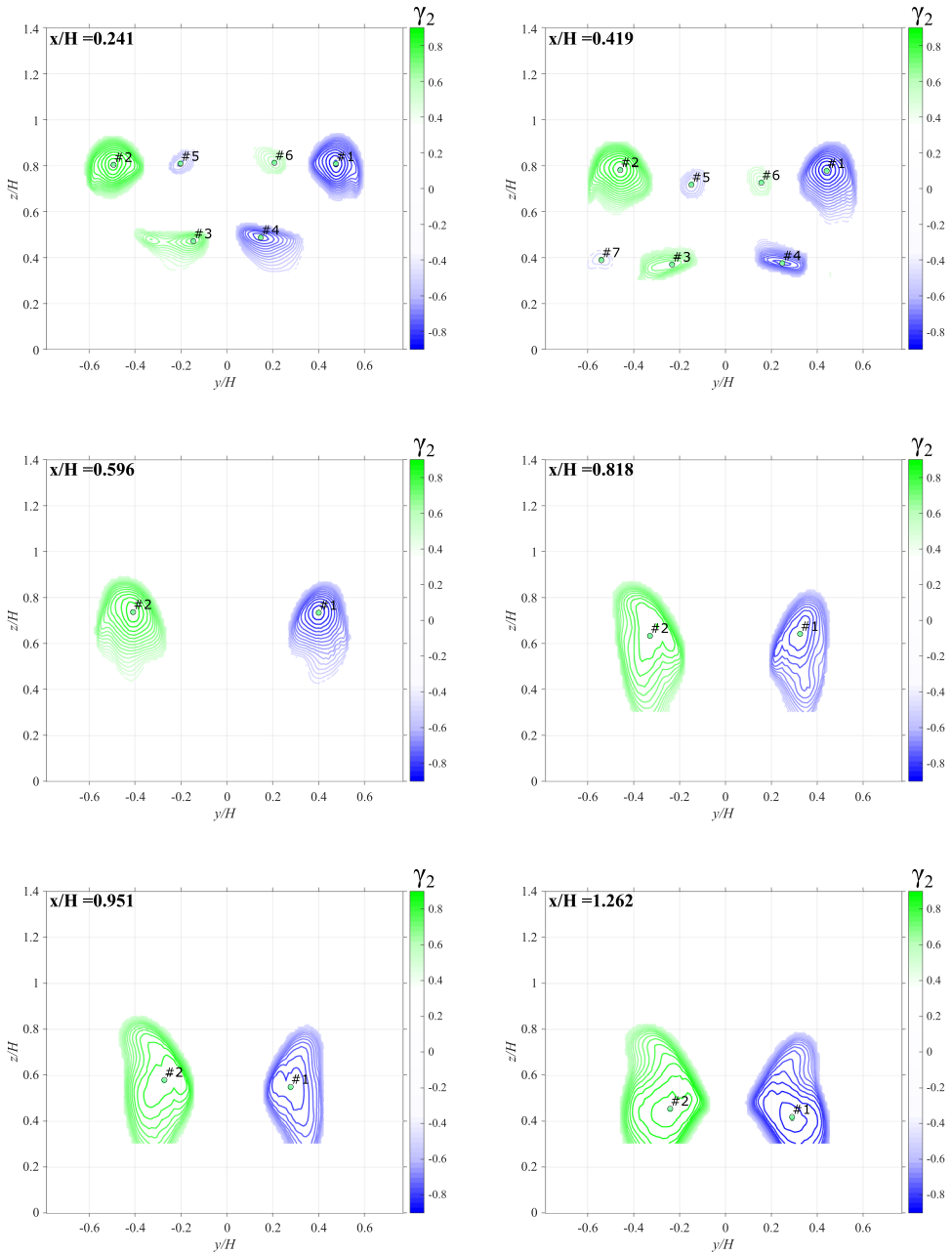

Fig. 11 Near-body wake slices of Ahmed body showing γ_2 contours and consistent vortex labels

5 Conclusions

A novel machine learning inspired approach has been introduced to tackle the problem of temporal and spatial coherent structure (vortex) tracking. The algorithm is capable of tracking multiple coherent structures robustly.

The γ_2 vortex detection approach described by Graftieaux et al. (2001) is first used to identify bounding contours around vortices in planar slices of a given flowfield. A *single-link* cluster method is then applied to group centroids of γ_2 contours together providing robust vortex centre determination. *Hungarian* assignment is then uniquely applied as a way to produce consistently labelled vortices.

The approach has been used to successfully demonstrate temporal and spatial vortex labelling and tracking. An example of the algorithm's ability to robustly handle a vortex merging phenomenon is demonstrated using a synthetic flowfield of Batchelor vortices. A volumetric, robotic PIV dataset of the flow in the wake of an Ahmed body is used to demonstrate the ability of the algorithm

to handle complex three-dimensional flowfields where the vortices have 3D trajectories.

Acknowledgements The authors would like to acknowledge Edoardo Saredi from TU Delft for processing the Ahmed body data. Nicholas Chester, Dirk De Beer and Simon Hine are also thanked for supporting the publication of this work.

References

Agüera N, Cafiero G, Astarita T, Discetti S (2016) Ensemble 3d PTV for high resolution turbulent statistics. Meas Sci Technol 27(12):1240111

Ahmed SR, Ramm G, Faltin G (1984) Some salient features of the time-averaged ground vehicle wake. SAE Tech 840300

Amsallam D, Zahr MJ, Farhat C (2012) Nonlinear model order reduction based on local reduced-order bases. Int J Numer Meth Eng 10:891–916

Azijli I, Dwight RP (2015) Solenoidal filtering of volumetric velocity measurements using gaussian process regression. Exp Fluids 56:198

Batchelor GK (1964) Axial flow in trailing line vortices. J Fluid Mech 20(4):645–658

de Bruin AC, Hegen GH, Rohne PB, Spalart PR (1996) Flow field survey in trailing vortex system behind a civil aircraft model at high lift. Technical report NLR TP 96284, National Aerospace Laboratory, NLR

Brunton SL, Noack BR, Koumoutsakos P (2019) Machine learning for fluid mechanics. Annu Rev Fluid Mech 52:1–31

Chong MS, Perry AE, Cantwell BJ (1990) A general classification of three-dimensional flow fields. Phys Fluids A 2(5):765–777

Cucitore R, Quadrio M, Baron A (1999) On the effectiveness and limitations of local criteria for the identification of a vortex. Eur J Mech B Fluids 18:261–282

Deng L, Wang Y, Chen C, Liu Y, Wang F, Liu J (2020) A clustering-based approach to vortex extraction. J Vis 1–16

Deng L, Wang Y, Liu Y, Wang F, Li S, Liu J (2019) A CNN-based vortex identification method. J Vis 22(1):65–78

Dinits EA (1970) Algorithm for solution on a problem on maximum flow in a network with power estimation. Sov Math Doclady 11:1277–1280

Edmonds J, Karp RM (1972) Theoretical improvements in algorithmic efficiency for network flow problems. J ACM 19:248–264

Graftieaux L, Michard M, Grosjean N (2001) Combining PIV, pod and vortex identification algorithms for the study of unsteady turbulent swirling flows. Meas Sci Technol 12:1422–1429

Gunther T, Theisel H (2017) The state of the art in vortex extraction. Comput Graph Forum 1981:1–24

Haller G, Hadjighasem A, Farazmand M, Huhn F (2016) Defining coherent vortices objectively from the vorticity. J Fluid Mech 795:136–173

Hardin JC, Wang FY (2003) Sound generation by aircraft wake vortices. Technical report CR-2003-212674, NASA

Hunt JCR, Wray AA, Moin P (1988) Eddies, streams and convergence zones in turbulent flows. Technical Report N89-24555, NASA Center for Turbulence Research

Jeong J, Hussain F (1995) On the identification of a vortex. J Fluid Mech 285:69–94

Jux C, Sciacchitano A, Schneiders JFG, Scarano F (2018) Robotic volumetric PIV of a full-scale cyclist. Exp Fluids 74:1–15

Kaiser E, Noack BR, Cordier L, Spohn A, Segond M, Abel M, Niven RK (2014) Cluster-based reduced-order modelling of a mixing layer. J Fluid Mech 754:365–414

Kim B, Gunther T (2019) Robust reference frame extraction from unsteady 2d vector fields with convolutional neural networks. Comput Graph Forum 38(3):285–295

Kline SJ, Robinson SK (1990) Turbulent boundary layer structure: progress, status and challenges. Struct Turbulen Drag Reduct 3–32

Kuhn HW (1955) The Hungarian method for the assignment problem. Naval Res Logist Q 2:83–97

Lignarolo LEM, Ragni D, Scarano F, Ferreira CJS, van Bussel GJW (2015) Tip-vortex instability and turbulent mixing in wind-turbine wakes. J Fluid Mech 781:467–493

Lugt HJ (1979) The dilemma of defining a vortex. In: Muller U, Roesner KG, Schmidt B (eds) In recent developments in theoretical and experimental fluid mechanics. Springer, New York, pp 113–138

Lumley JL (1981) Coherent structures in turbulence. In: Meyer RE (ed) Transition and turbulence. Academic Press Inc., Canvridge, pp 215–242

Manning CD, Raghaven P, Schütze H (2008) In: Introduction to information retrieval. Cambridge University Press

Munkres J (1957) Algorithms for the assignment and transportation problems. J Soc Ind Appl Math 5:32–38

Scarano F, Ghaemi S, Caridi GCA, Bosbach J, Dierksheide U, Sciacchitano A (2015) On the use of helium-filled soap bubbles for large-scale tomographic PIV in wind tunnel experiments. Exp Fluids 56(2):42

Schanz D, Gesemann S, Schroder A (2016) Shake-the-box: Lagrangian particle tracking at high particle image densities. Exp Fluids 57(5):1–27

Schneiders JFG, Scarano F, Jux C, Sciacchitano A (2018) Coaxial volumetric velocimetry. Meas Sci Technol 29(6):065201

Sciacchitano A, Giaquinta D (2019) Investigation of the ahmed body cross-wind flow topology by robotic volumetric PIV. In: Proceedings of the 13th international symposium on particle image velocimetry: 22–27 July, Munich, Germany, vol 13, pp 311–320

Sciacchitano A, Scarano F (2014) Elimination of PIV light reflections via a temporal high pass filter. Meas Sci Technol 25(8):084009

Sibson R (1972) An optimally efficient algorithm for the single-link cluster method. Comput J 16(1):30–34

Simpson CE, Babinsky H, Harvey JK, Corkery S (2018) Detecting vortices within unsteady flows when using single-shot PIV. Exp Fluids 59:125

Spalart PR (1988) Direct simulation of a turbulent boundary layer up to rtheta = 1410. J Fluid Mech 187:61–98

Spencer NH (2013) In: Essentials of multivariate data analysis. CRC Press, Boca Raton FL, pp 91–95

Wang Y, Deng L, Yang Z, Zhao D, Wang F (2021) A rapid vortex identification method using fully convolutional segmentation network. Vis Comput 37:261–273

Xu R, Wunsch D (2008) Clustering, vol 10. Wiley, New York, pp 1–358

Zhang X, Toet W, Zerihan J (2006) Ground effect aerodynamics of race cars. Appl Mech Rev 59(1):33–49

Zhou J, Adrian RJ, Balachandar S, Kendall TM (1999) Mechanisms for generating coherent packets of hairpin vortices in channel flow. J Fluid Mech 387:353–396